THE JOURNAL OF PHYSICAL CHEMISTRY B

Article

pubs.acs.org/JPCB

Oxidative Interaction between OxyHb and ATP: A Spectroscopic Study

Mousumi Banerjee,[†] Abhijit Chakrabarti,[‡] and Samita Basu*[,†]

[†]Chemical Sciences Division and [‡]Structural Genomics Division, Saha Institute of Nuclear Physics, 1/AF Bidhannagar, Kolkata 700064, India

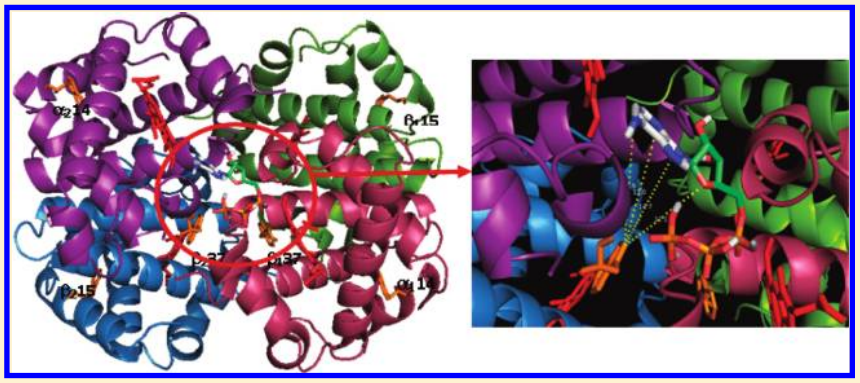

ABSTRACT: The binding mode between oxyhemoglobin (oxyHb) and adenosine triphosphate (ATP) has been studied using absorption and fluorescence spectroscopy. OxyHb forms a ground state complex with ATP supported by five isosbestic points which appear in absorption spectra of oxyHb in buffer solution on addition of ATP. Moreover, the changes in absorption spectra suggest an oxidative interaction between the particular interacting systems. The binding constant has been determined from the quenching of fluorescence of oxyHb in the presence of a varied concentration of ATP, and that is 3.8×10^3 M^{-1} at 25 °C. The negative changes in entropy and enthalpy indicate that the binding is enthalpy driven and the hydrogen bond and van der Waals (stacking) interactions play a major role. The oxygen affinity of oxyHb decreases with simultaneous formation of metHb in the presence of ATP. ATP-induced structural changes have been affirmed using both circular dichroism spectroscopy and synchronous fluorescence. A theoretical docking study gives the molecular details about the binding site of ATP in oxyHb.

1. INTRODUCTION

Human hemoglobin (HbA) (Figure 1), the major protein component in erythrocytes, usually covers one-third the volume

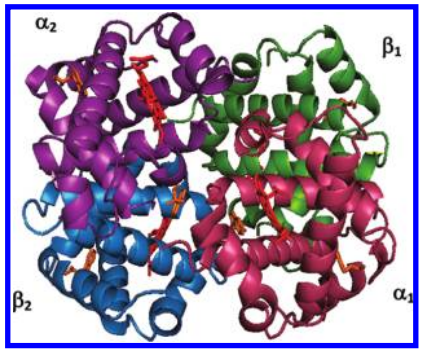

Figure 1. Structure of tetrameric hemoglobin.

of an individual cell. It exists as a tetramer of the globin chains, which is composed of two α and two β subunits, and each α- and β-subunit contains 141 and 146 amino acid residues, respectively. The relationship between the structure and function of Hb inside cells is well established.[1−4] Hb is an important functional protein as reversible oxygen carrier and storage.[5] Three types of intrinsic fluorophores are present in Hb. They are tryptophan, tyrosine, and phenylalanine. Six tryptophan residues are found in tetrameric hemoglobin.

A significant amount of adenosine 5′-triphosphate (ATP) (Figure 2) is present in human erythrocytes[6] and affects the O_2-

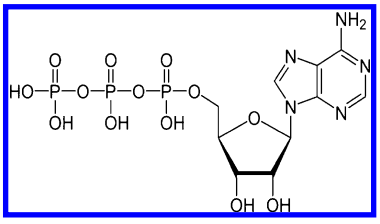

Figure 2. Molecular structure of adenosine 5′-triphosphate.

affinity and structure of Hb.[7,8] ATP converts oxyHb to deoxyHb reversibly and binds preferably with metHb. The interactions between ATP and different types of Hb were studied extensively.[9−12] The O_2 affinity of oxyHb is suppressed

Received: March 27, 2012
Revised: May 7, 2012
Published: May 8, 2012

dx.doi.org/10.1021/jp302899t | J. Phys. Chem. B 2012, 116, 6150−6157

by ATP in the case of human and other classes of Hb. ATP mainly binds at the organic phosphate binding site of Hb.[9] There are two binding sites present within Hb with binding constants of the order of 10^9 and 10^5 M^{-1}, respectively, with ATP. There is one more binding constant for oxyHb of the order of 10^3 M^{-1} in the presence of an excess of complexing anions.[10] The extent of the oxygen affinity of oxyHb depends on environment. For example, it decreases in the presence of ATP. When oxyHb is converted to metHb, its tertiary and quaternary structural changes are observed.[11−13] An X-ray crystallographic study on normal Hb demonstrated that during deoxy to oxyHb transition a large movement takes place at the $\alpha_1\beta_2$ contact.[14] The focus of our present study is to find out the binding and conformational changes of Hb after binding with ATP using steady-state and time-resolved fluorescence and CD, although several other processes were already adopted by others to study the binding interaction between Hb and ATP.

ATP is a common neucleoside triphosphate in both deoxyriboneucleic acid (DNA) and ribonucleic acid (RNA). The basic difference is the presence of a hydroxyl group at the 2′ position of ATP in the case of RNA which is not found in DNA. Actually, ATP is one of the basic units of the macromolecules, DNA and RNA. Therefore, the interaction modes between ATP and blood protein Hb throw some light on the interactions between DNA and protein as well as RNA and protein on a larger scale which are important in protein and DNA functions *in vivo*. Protein−RNA and protein−DNA interactions occur mainly through electrostatic interactions, hydrogen bonding formation, hydrophobic interactions, and base stacking. Therefore, in the present system, knowledge on the mode of binding between Hb and ATP is very important to find out the actual interactions which play a major role between Hb and nucleoside phosphate ATP.

In this paper, we have presented details of absorption and fluorescence measurements of the bimolecular interaction of ATP with oxyHb in aqueous solution. Steady-state and time-resolved fluorescence intensities of oxyHb as a function of ATP concentration provide the nature of quenching and binding using Stern−Volmer and Van't Hoff plots, respectively. The structural changes have been observed by CD and synchronous fluorescence spectra of Hb with varied concentrations of ATP.

2. MATERIALS AND METHODS

2.1. Reagents. Tris and adenosine 5′-triphosphate were purchased from Sigma-Aldrich, USA. All buffer solutions were prepared in triply distilled water.

2.2. Isolation and Purification of Hemoglobin from Human Blood Samples. Hb was purified from the blood sample collected from normal volunteers with Hb count 13.6 g/dl. Human erythrocytes, after removal of the buffy coat and plasma, were extensively washed with phosphate-buffered saline (5 mM phosphate, 0.15 M NaCl, pH 7.4). Hb was isolated from packed erythrocytes by osmotic lysis using three volumes of 1 mM Tris, pH 8.0, at 4 °C for 1 h. The hemoglobin mixture was purified by gel filtration on a Sephadex G 100 column (30 × 1 cm) in a buffer containing 5 mM Tris and 50 mM KCl with pH 8.0. The Hb sample was stored in oxy-format −70 °C for less than 7 days and characterized by the measurements of absorption at 415 and 541 nm, respectively. The purity of the Hb preparations was checked by 15% SDS-PAGE after staining with Coomassie blue. Densitometry analysis (Quantity One software, Bio-Rad USA) indicated the Hb preparations to be >90% pure. The protein concentration was determined spectrophotometrically using a molar extinction coefficient of 125 000 M^{-1} cm^{-1} at 415 nm and 13 500 M^{-1} cm^{-1} at 541 nm, respectively.[15]

2.3. Absorption Measurements. The absorption spectra have been recorded on a JascoV-650 absorption spectrophotometer over a wavelength range from 250 to 600 nm. A 1 cm path length cuvette has been used. In this experiment, first 2 mL of 11 × 10^{-6} M (per heme basis) oxyHb has been placed in a sample chamber along with the same volume of buffer in the reference cell and the absorption spectrum has been recorded. Then, the ATP aliquot has been added sequentially in both reference and sample chambers in a calculated amount over the concentration range from 0 to 8 × 10^{-4} M to observe mainly the effect of only complex formation between oxyHb and ATP.

The spectral changes of oxyHb between 500 and 700 nm suggest the loss of oxyHb species and formation of metHb, indicating interaction between hemoglobin species and ATP. The concentrations of different oxidized Hb species were determined before by using four component analysis methods.[16] The equation is

$$[\text{oxyHb}] = 119 \times A_{577} - 39 \times A_{630} - 89 \times A_{560} \quad (1)$$

To study the extent of loss of oxyHb with varying concentrations of ATP has been calculated as follows:

$$\text{oxyHb}\ (\%) = \{[\text{oxyHb}]_n/[\text{oxyHb}]_0\} \times 100 \quad (2)$$

where $[\text{oxyHb}]_n$ is the concentration of oxyHb at different ATP concentrations and $[\text{oxyHb}]_0$ is the initial concentration of oxyHb before addition of ATP.

2.4. Fluorescence Measurements. Steady-state fluorescence measurements between 310 and 500 nm with an excitation wavelength of 280 nm have been performed with a Hitachi-7000 spectrophotometer. The cuvette path length was 1 cm. The excitation and emission band passes have been fixed at 2.5 and 5 nm, respectively. The concentration of oxyHb has been kept at 4 × 10^{-6} M, and the ATP concentration has been varied from 0 to 15 × 10^{-5} M for fluorescence quenching experiments.

2.5. Stern−Volmer Plot for Fluorescence Quenching. The quenching of fluorescence has been analyzed using the following Stern−Volmer equation:[17]

$$\frac{F_0}{F} = 1 + K_{SV}[Q] \quad (3)$$

where F_0 and F are the relative fluorescence intensities in the absence and presence of quencher, respectively, K_{SV} is the Stern−Volmer constant, and [Q] is the concentration of the quencher.

$$K_{SV} = k_q\tau_0 \quad (4)$$

where k_q is the bimolecular quenching rate constant and τ_0 is the average lifetime of oxyHb in the absence of ATP. k_q comes from the given equation

$$k_q = 4\pi aDN_A \times 10^{-3} \quad (5)$$

where D is the sum of diffusion coefficients of fluorophore and quencher, a is the sum of molecular radii, and N_A is Avogadro's number.

2.6. Measurements of Lifetime by Time-Correlated-Single-Photon Counting Device. Fluorescence lifetimes have been measured using a time-correlated-single-photon counting (TCSPC) spectrophotometer (Horiba Jobin Yovin)

dx.doi.org/10.1021/jp302899t | J. Phys. Chem. B 2012, 116, 6150−6157

with FWMH ~ 790 ps and repetition rate 1 MHz. The excitation and emission wavelengths have been chosen to be 280 and 326 nm, respectively.

2.7. Estimation of Binding Constant. The binding parameters, i.e., binding affinity constant and binding stoichiometry for the interaction between oxyHb and ATP have been estimated from the quenching of protein fluorescence at maximum emission at 326 nm with excitation at 280 nm on subsequent addition of ATP. The quenching data have been analyzed to determine the binding affinity constant (K_a) following the relation below[18,19]

$$\frac{1}{\Delta F} = \frac{1}{\Delta F_{max}} + \frac{1}{\Delta F_{max} \cdot K_a} \cdot \frac{1}{L} \quad (6)$$

where $\Delta F = F_0 - F$ and F_0 and F denote the protein fluorescence in the absence and presence of the ligand (L), respectively. ΔF_{max} represents the maximum quenched fluorescence intensity obtained from the intercept of the linear plot of $1/\Delta F$ against $1/L$. ΔF_{max} has been determined from the intercept, and the slope gives the value of the binding affinity constant (K_a).

2.8. Analysis of Thermodynamic Parameters. The thermodynamic parameters for ATP binding with oxyHb have been determined from the van't Hoff equation:

$$\ln K_a = -\frac{\Delta H^0}{RT} + \frac{\Delta S^0}{R} \quad (7)$$

where K_a is the binding affinity constant at corresponding temperature T and R is the gas constant. The equation gives the standard enthalpy change (ΔH°) and standard entropy change (ΔS°) on binding. The free energy change (ΔG°) has been estimated from the following relationship:

$$\Delta G^\circ = \Delta H^\circ - T\Delta S^\circ \quad (8)$$

2.9. Measurements of Circular Dichroism (CD). The far-UV and near-UV CD spectra have been measured on a Jasco-720. The CD spectra of oxyHb have been recorded in the absence and presence of ATP using a 1 mm path length cuvette within the wavelength range 190−250 nm and 1 cm path length cuvette within the range 240−320 nm. The CD results have been analyzed in terms of mean residue ellipticity (MRE) in deg·cm^2·dmol^{-1} according to the following equation:[20]

$$[\theta_\lambda] = \frac{\mu\theta}{10LC} \quad (9)$$

where C is the concentration of Hb in g/mL, θ is observed rotation in degree, L is the path length in cm, and μ is the mean residual molecular weight of protein.

Quantitative assessment of the percentage of α-helix in oxyHb in the presence and absence of ATP can be estimated by the relation of Chen et al:[21,22]

$$\%\ \text{of}\ \alpha\text{-helix} = \frac{[\theta]_{222} + 2340}{-30300} \quad (10)$$

$$\%\ \text{of}\ \alpha\text{-helix} = \frac{[\theta]_{208+4000}}{33000 - 4000} \quad (11)$$

where $[\theta]_{222}$ and $[\theta]_{208}$ are the observed MRE value at 222 and 208 nm, respectively. In eq 10, 2340 is the MRE of the β-form and random coil conformation cross at 222 nm and 30 000 is the pure helix at 222 nm. Similarly, in eq 11, 4000 is the MRE of the β-form and random coil conformation cross at 208 nm and 33 000 is the pure α-helix at 208 nm.

2.10. Molecular Docking Studies. A theoretical view of the Hb and ATP has been established by using a docking study. The crystal structure of Hb (PDB entry 2DN1)[23] has been downloaded from the Protein Data Bank. The Online Docking Server (http://www.dockingserver.com) has been used to perform the docking calculations. The computational method used by the server is the following. The Dreiding force field is used for energy minimization of ligand molecule using built-in Chemaxon tools in the Docking Server. The Gasteiger partial charges are added to the ligand atoms. Nonpolar H atoms are merged, and rotable bonds are defined. Essential H atoms, Kollman united atom type charges, and solvation parameters are added with the aid of AutoDock tools. Affinity (grid) maps of 52 × 52 × 48 Å grid points and 1 Å spacing are generated using the Autogrid program. The AutoDock parameter set and distance-dependent dielectric functions are used in the calculation of the van der Waals and electrostatic terms, respectively. Docking simulations are performed using the Lamarckian genetic algorithm (LGA)[24−27] and the Slis and Wets local search method. Initial position, orientation, and torsions of the ligand molecules are set randomly. Each docking experiment is derived from 10 different runs that are set to terminate after a maximum of 250 000 energy evaluations. The population size is set to 150. During the search, a translational step of 0.2 Å and quaternion and torsion steps of 5 are applied. The output from autoDock is rendered with PyMOL.[28] Here, PyMOL has also been used to calculate the distances between nearest atoms which interact with each other.

The accessible surface areas (ASA) of uncomplexed (only Hb) and complexed (Hb with ATP) protein have been calculated from the Helix Systems server. The protein−ligand structure corresponding to the minimum score as obtained from the AutoDock Vina analysis has been chosen.[28] The change in ASA for each residue has been calculated using $\Delta ASA = ASA_{Hb} - ASA_{Hb\text{-}ATP}$.

3. RESULTS AND DISCUSSION

3.1. Absorption Measurements. Figure 3a shows the absorption spectra of oxyHb in buffer where some significant changes are observed on addition of ATP. There are two notable points which are the existence of five isosbestic points (at 409, 353, 477, 521, and 587 nm) and the decrease in absorbance of the Q-band of oxyHb (R) at 541 and 576 nm, as shown in the inset of Figure 3a. The observations signify the formation of the ground state complex between oxyHb and ATP which decreases the oxygen affinity of oxyHb with increasing concentration of ATP. The isosbestic point at 587 nm, according to previous literature,[29] signifies the formation of metHb that infers the preference of binding of ATP to another form of oxyHb, i.e., metHb. Figure 3b depicts that the absorbance of oxyHb at 415 nm decreases gradually with simultaneous increase of another peak at 630 nm on addition of ATP. This result indicates that in the presence of ATP autoxidation of oxyHb occurs and oxyHb is converted to metHb where Fe (+2) goes to the Fe (+3) state. The percentage of autoxidation of oxyHb in the presence of ATP has been calculated according to eqs 1 and 2, which shows the changes of oxyHb from 100 to 86% favoring its autoxidation in the presence of ATP. This is the first report based on spectroscopic observations regarding the capacity of ATP to induce transition in oxyHb among its different states.

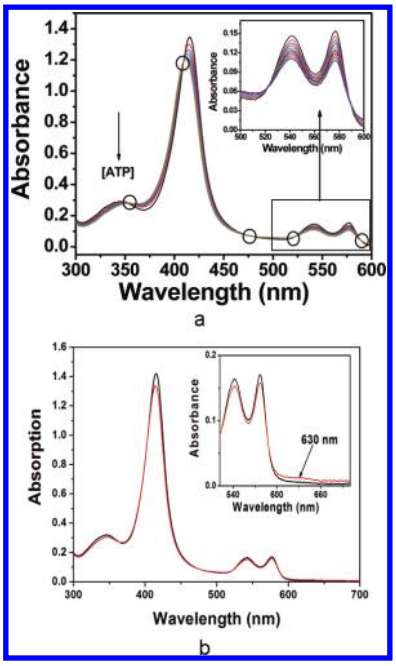

Figure 3. (a) Absorption spectra of 11 × 10^{-6} M oxyHb with increasing concentration of ATP from 0 to 8 × 10^{-4} M. The inset shows the magnified absorption spectra ranging from 500 to 600 nm. (b) Absorption spectra of oxyHb (11 × 10^{-6} M) in absence and presence of ATP (2 × 10^{-4} M). The inset shows the magnified absorption spectra ranging from 520 to 700 nm.

3.2. Fluorescence Measurements. The interaction between oxyHb and ATP has been studied fluorometrically by quenching the intrinsic fluorescence of the Trp residues of Hb with sequential addition of ATP. The steady state fluorescence spectra of Hb show a peak at 326 nm (Figure 4). Normal Trp in aqueous environment shows a peak at 350

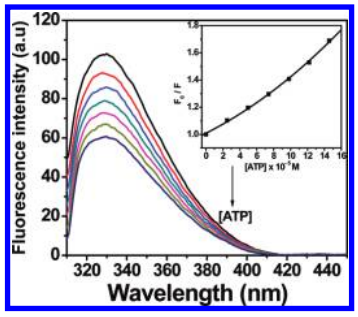

Figure 4. Fluorescence spectra of 4 × 10^{-6} M oxyHb with increasing concentration of ATP from 0 to 15 × 10^{-5} M; the excitation and emission wavelength are fixed at 280 and 326 nm, respectively. OxyHb was kept in 20 mM Tris buffer at pH 7.4. The inset shows the Stern–Volmer plot for fluorescence quenching of oxyHb with a varying concentration of ATP.

nm; however, inside the hydrophobic environment of proteins, the peak is blue-shifted. For normal oxyHb, this blue shift of the fluorescence peak of Trp from 350 to 326 nm is significant. Moreover, the fluorescence intensity of Hb is very weak because of the occurrence of intramolecular FRET between Trp and the heme moiety inside oxyHb. Although there are 6 Trp residues, β37 Trp has a significant contribution toward the fluorescence of Hb. In the presence of ATP, the fluorescence of oxyHb quenches gradually. The Stern–Volmer plot based on the quenching data has been obtained (Figure 4, inset). The plot displays a nonlinear upward bending toward the F_0/F axis with an increase in concentration of ATP. There may be several reasons behind the nonlinearity in the Stern–Volmer plot, e.g., presence of both static (ground state) and dynamic (excited state) quenching, ionic nature of the interacting molecules, presence of more than one Trp residue in the protein, etc.[21] However, the changes in the absorption spectrum of oxyHb in the presence of ATP indicate a static type of quenching that occurs between oxyHb and ATP. In the case of oxyHb, only β37 Trp is functioning and its fluorescence is quenched by ATP. Therefore, although Hb has 6 Trp, the reason of differential accessibility of Trp moieties toward nonlinearity in the Stern–Volmer plot is least probable. However, the charges on ATP in neutral pH medium might be one of the causes for such nonlinearity.[17]

The time-resolved fluorescence analysis gives the average lifetime of oxyHb as 2.2 ns, as already been reported.[30] The lifetime does not decrease significantly with gradual addition of different concentrations of ATP. With the help of K_{SV} and fluorescence lifetime (τ_0) values, a k_q value has been determined from eq 4 which is 1.449 × 10^{12} M^{-1} s^{-1}. The upper limit of k_q is 10^{10} M^{-1} s^{-1} for a diffusion control phenomenon from eq 5,[31] which indicates that the quenching is static in nature, suggesting the formation of a ground state complex.

3.3. Binding Constant Determination. The binding association constant (K_a) has been determined from steady state fluorescence quenching experiments. The K_a value has been calculated from the Benesi–Hildebrand plot[31,32] as 3.8 × 10^3 M^{-1} at 25 °C. The binding constant has been found to decrease with increasing temperature (Table 1, Figure 5), which also suggests that a ground state complex is formed between oxyHb and ATP.

Table 1. Binding Constant and Thermodynamic Parameters at Four Different Temperatures

temperature (K)	association constant × 10^3 (M^{-1})	$\Delta H°$ (kJ mol^{-1})	$\Delta S°$ (J mol^{-1} K^{-1})	$\Delta G°$ (kJ mol^{-1})
293	4.5	−60.30	−135.15	−20.75
298	3.8			−20.07
303	2.1			−19.39
308	1.4			−18.72

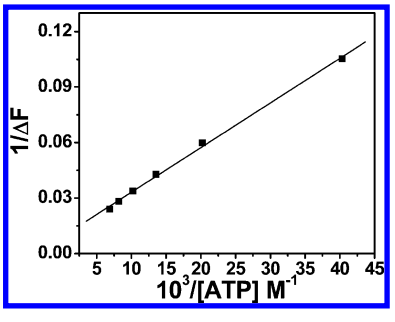

Figure 5. Double reciprocal plot of $1/\Delta F$ against $1/[ATP]$ to evaluate the binding affinity constant K_a of oxyHb with ATP in the 20 mM Tris buffer, pH 7.5 at 298 K. The oxyHb concentration was kept at 4 × 10^{-6} M and ATP (0–15) × 10^{-5} M.

dx.doi.org/10.1021/jp302899t | J. Phys. Chem. B 2012, 116, 6150–6157

3.4. Thermodynamic Studies. The nature of interactions between protein and drug molecules has been predicted from the thermodynamic parameters of binding, i.e., changes in standard enthalpy, entropy, and Gibb's free energy. There are four types of interactions, i.e., H-bonds, van der Waal's forces, electrostatic interactions, and/or hydrophobic interactions. From the $\ln K_a$ vs $1/T$ plot, commonly known as the van't Hoff plot (Figure 6 and eqs 7 and 8), the values of $\Delta H°$, $\Delta S°$,

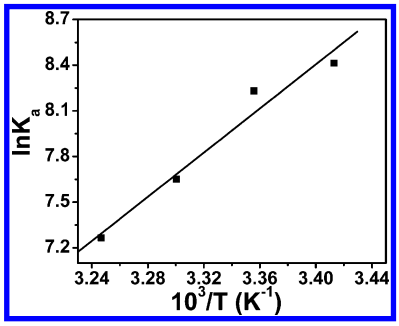

Figure 6. van't Hoff plot of $\ln K_a$ vs $1/T$ for the binding of oxyHb (4×10^{-6} M) with ATP in the same Tris buffer, pH 7.4, at four different temperatures.

and $\Delta G°$ have been calculated as -60.30 kJ mol^{-1}, -135.15 J K^{-1} mol^{-1}, and -20.07 kJ mol^{-1}, respectively, at 25 °C. The decrease in entropy and enthalpy suggests that the interaction between Hb and ATP is an enthalpy driven process and the H-bonding, van der Waal's type of interactions are the main involving factors. Literature data also suggest that any molecule resembling the structure of ATP undergoes stacking interactions with proteins.[17]

3.5. Synchronous Fluorescence. The conformational changes of oxyHb in the presence of ATP have been studied by synchronous fluorescence spectroscopy that involves simultaneous scanning of the excitation and emission monochromators, maintaining a constant wavelength interval between them. The synchronous fluorescence spectroscopy gives information about the microenvironment of the chromospheres such as Trp and Tyr as amino acid residues in the case of proteins. This technique has several advantages. It can simplify the spectrum, reducing its bandwidth and increasing sensitivity avoiding different perturbing effects.[5] Usually, each protein has only one emission band in the normal fluorescence spectrum, which is due to the emission of both Trp and Tyr because their emission peaks merge in the normal fluorescence spectroscopy. In order to distinguish the emission peaks of Trp and Tyr residues, the synchronous fluorescence spectroscopic technique has been used. It was reported that the shorter wavelength difference ($\Delta\lambda$ = 30 nm) signifies the microenvironment of Tyr residues and the longer wavelength difference ($\Delta\lambda$ = 80 nm) indicates the microenvironment of Trp residues.[5,33]

The fluorescence spectra of the Tyr and Trp residues of oxyHb at various concentrations of ATP have been shown in Figure 7a where the peak at 335 nm for the Tyr residue is red-shifted to 343 nm. The Trp microenvironment is very much sensitive toward polarity, because with increasing concentration of ATP the peak at 315 nm totally disappears and the 355 nm peak intensity increases. The 355 nm peak is due to the tryptophan in aqueous solution alone. Such changes suggest the decrease in hydrophobicity of Trp and Tyr in the presence of ATP (Figures 7 and 8).

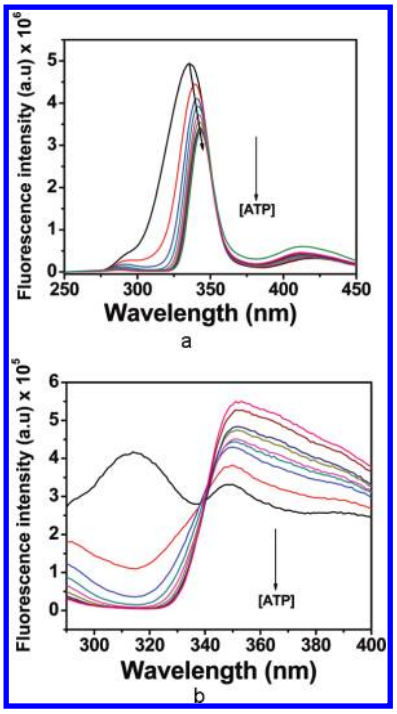

Figure 7. Synchronous fluorescence spectrum of oxyHb (T = 293 K, pH 7.4). [oxyHb] = 8×10^{-6} M. ATP concentrations for the ATP–Hb system (from up to down) were 0, 1, 1.5, 2.4, 3, 4, 4.6, 5.2, and 6.1 $\times 10^{-4}$ M: (a) $\Delta\lambda$ = 30 nm; (b) $\Delta\lambda$ = 80 nm.

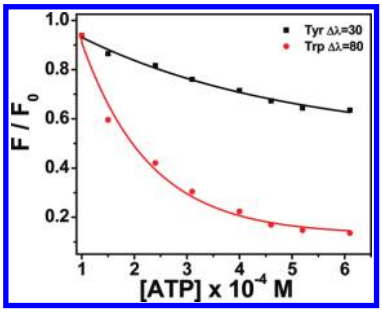

Figure 8. The quenching of oxyHb synchronous fluorescence by ATP. [oxyHb] = 8×10^{-6} M. (■) $\Delta\lambda$ = 30 nm, (●) $\Delta\lambda$ = 80 nm.

The Hb contains three Trp residues in each $\alpha\beta$ dimer, i.e., a total of six in the tetramer. These six residues are two of each of α-14Trp, β-15Trp, and β-37Trp. The α-14Trp and β-15Trp residues are present outside the subunit interface,[34] and the β-37 Trp residue is located at the $\alpha_1\beta_2$ interface, which was assigned as the primary source of fluorescence emission.[35] The amino acid residues α-42Tyr, α-140Tyr, and β-145Tyr are also located at the $\alpha_1\beta_2$ interface.[36] The red shift and increasing intensity at the 355 nm peak observed in Figure 7 are consistent with rearrangement of the tertiary structure of Trp and Tyr residues during the binding process. It has also been shown in Figure 8 that the slope of the plot F/F_0 vs ATP concentration is more for $\Delta\lambda$ = 80 nm than $\Delta\lambda$ = 30 nm, indicating that ATP can change the tertiary conformation of oxyHb and mainly the surrounding polarity of Trp rather than that of Tyr.

3.6. Circular Dichroism Spectroscopy. The conformational changes of Hb at the secondary, tertiary, and quaternary structural levels have been assigned by far- and near-UV CD spectra. The far-UV CD spectral range is from 200 to 250 nm,

dx.doi.org/10.1021/jp302899t | J. Phys. Chem. B 2012, 116, 6150–6157

which indicates the secondary backbone structural changes of Hb in the absence and presence of ATP (Figure 9). From eqs 9,

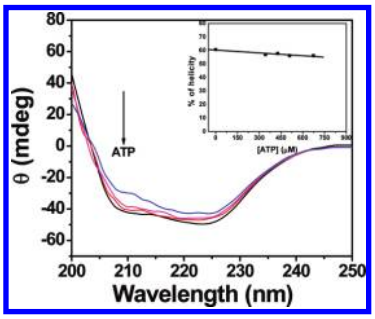

Figure 9. The far-UV circular dichroism spectra (200–250 nm) of pure oxyHb (8×10^{-6} M) and in the presence of an increasing concentration of ATP in 20 mM Tris buffer, pH 7.4. The spectra were presented as an average of five scans. The inset shows the % α-helicity of oxyHb in the presence of 0, 3, 4, 5, and 7×10^{-4} M ATP.

10, and 11, the percentage of α-helicity has been calculated, which is 83% for only Hb. With increasing concentration of ATP, the helicity changes to 71% at 222 nm. This observation indicates the occurrence of a secondary structural change to some extent when oxyHb undergoes complexation with ATP. This % helicity change suggests some backbone conformational changes rather than unfolding of suggested protein in the presence of proposed small molecule ATP.

The near-UV CD spectra give information about the contributions of aromatic side chains and disulfide bonds.[37] The tertiary and quaternary structural changes occur when oxyHb converts to metHb, i.e., from the R- to T-form.[37] The α-42Tyr, α-140Tyr, β-37Trp, and β-145Tyr residues are located at the $\alpha_1\beta_2$ interface, and the environmental changes are found for these amino acid residues during oxy to met conversion in the presence of ATP. In Figure 10, a distinct positive peak has

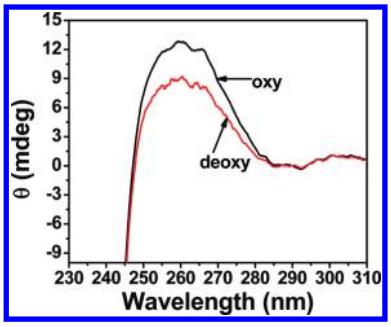

Figure 10. The near UV circular dichroism spectra of oxyHb (16×10^{-6} M) in the presence of 5×10^{-4} M ATP ranging from 230 to 310 nm.

been found at 260 nm which is strictly influenced by the attached ligand, thereby the spin state of the iron atom. In the presence of ATP, the 260 nm peak deceases for oxy to met conversion due to changes of optical activity of the heme moiety in both α and β chains.[34,35] It indicates that tertiary structural changes occur during R to T transformation, which has already been crosschecked by the absorption and synchronous fluorescence spectra.

3.7. Docking Results. Docking results indicate that ATP binds at the surface of Hb. It prefers to bind between α_1–α_2 interfaces. Hb has six Trp residues: two Trp-α14, two Trp-β15, and two Trp-β37. Now the two β37 Trp residues are present in two different α–β interfaces. In this present docking study, among the six Trp residues, mainly Trp-$\beta_2$37 interacts with the small molecule ATP (Figure 11a). Other Trp residues are present in the hydrophobic core of the protein; therefore, these Trps are not accessible for the interacting ATP molecule. The small ATP molecule preferably binds to the surface of the Hb; therefore, it does not exist within the hydrophobic cavity of Hb. The thermodyanamic parameters calculated from experiments also suggest the fact that Hb-ATP interaction is mainly stacking type due to the planar moeity of adenosine present in ATP and Trp. There is no scope for major hydrophobic interaction of ATP in the interior region of protein Hb. Hence, the probability of differential accessibility of Trp toward ATP is not acceptable in this particular system. The accessible surface area of Hb is 23 360 Å^2, and the accessible area of the Hb–ATP complex is 23 304 Å^2. Thus, the accessible surface area of Hb changes when it binds with ATP. Now the ΔASA vs residue number plot shows huge changes in α_1 and β_2 subunits. The particular residue which shows maximum accessible surface area change is β_2-R40. Other important amino acid residues are α_1-P44, α_1-L91, β_2-F41, β_2-E43, and β_2-L96 (Figure 11b). From theoretical docking studies, the free energy change (ΔG°) of Hb–ATP interaction has been found to be −30 kJ mol^{-1}, which is quite larger compared to the experimental value. Actually, the docking analyses give the most probable energetically favored model of ATP bound Hb, which is dynamical and may not remain identical in the experimental conditions. Moreover, the docking studies show that the interaction of ATP is not with Trp alone but also with other aminoacids. Figure 11b depicts a prominent interaction between ATP and β_2-R40 of Hb. Another binding site of ATP is the rest of the Hb tetramer. Along with Trp β37, the Tyr α46 residue also interacts closely with ATP. Therefore, those may be the reasons behind the discrepancy in the values of (ΔG°) obtained theoretically and experimentally in this particular case.

4. CONCLUSION

The interaction between Hb and ATP was studied previously in different ways; however, in this paper, this interaction associated with conformational changes of oxyHb in the presence of ATP has been studied concurrently by spectroscopic methods. In the presence of ATP, the tertiary structure of oxy Hb significantly changes due to conversion of oxyHb to metHb which is clearly evident from absorption spectra of oxyHb in the presence of ATP. The ATP molecules facilitate autoxidation of oxyHb, converting it to metHb. Synchronous fluorescence also supports this phenomenon. The formation of a ground state complex as indicated by the existence of five isosbestic points in absorption spectra of oxyHb in the presence of ATP is the precursor of the conversion between oxyHb and metHb, as characterized by the decrease in absorbance of the Soret peak at 415 nm, Q bands of oxyHb at 541 and 576 nm, and formation of a new peak at 630 nm. Moreover, the nonlinearity in the Stern–Volmer plot and the decrease in binding association constants between oxyHb and ATP with temperature support the formation of the ground state complex. Actually, in the presence of ATP, the conformational changes between oxyHb and metHb increase with a decrease in oxygen affinity of the former. Theoretical docking study suggests that ATP binds at the α–β interface and β_2-R40 is interacting with maximum efficiency.

dx.doi.org/10.1021/jp302899t | J. Phys. Chem. B 2012, 116, 6150–6157

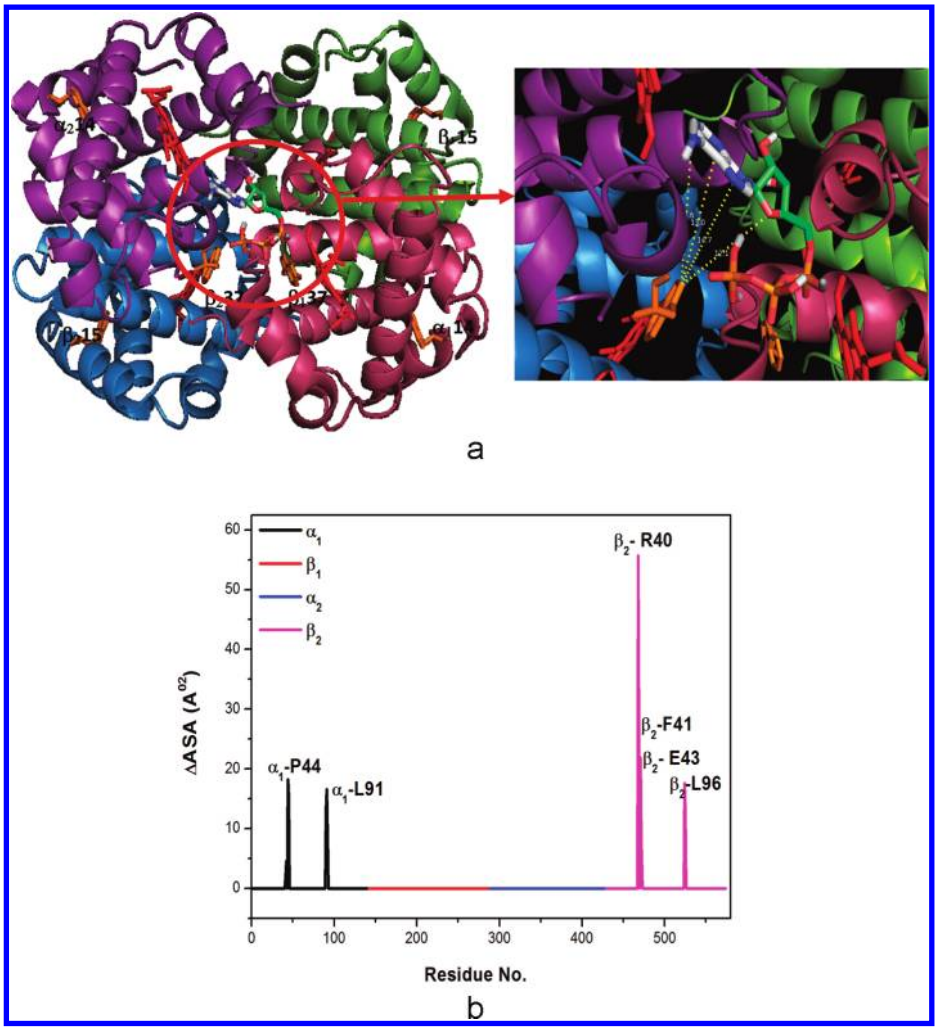

Figure 11. (a) Docking conformations of ATP in complex with Hb. Each subunit of Hb is colored differently (pink α_1, green β_1, violet α_2, blue β_2). ATP is multicolored (the reader is referred to the web version of the article). (b) The change in accessible surface area (ASA) (Å^2) for Hb plotted against amino acid residues.

AUTHOR INFORMATION

Corresponding Author

*E-mail: samita.basu@saha.ac.in. Phone: +91-33-2337-5345. Fax: +91-33-2337-4637.

Notes

The authors declare no competing financial interest.

ACKNOWLEDGMENTS

We are grateful to Mrs. Chitra Raha, SINP, Kolkata, for her assistance in laser flash photolysis experiments, Mr. Ajay Das SINP, Kolkata, for his assistance in fluorescence lifetime measurements, and Prof. Soumen Basak, Chemical Science Division, SINP, Kolkata, for his guidance during the CD measurements. We would also like to thank the "MMDDA" and "SPGHGD" project of SINP for financial support. We sincerely thank the reviewers for their valuable suggestions.

REFERENCES

(1) Lukin, J. A.; Ho, C. *Chem. Rev.* **2004**, *104*, 1219−1230.
(2) Imai, K.; Tsuneshige, A.; Harano, T.; Harano, K. *J. Biol. Chem.* **1989**, *264*, 11174−11180.
(3) Marengo-Rowe, A. J. *Proc (Bayl Univ Med Cent)* **2006**, *19*, 239−245.
(4) Nichols, W. L.; Zimm, B. H.; Ten Eyck, L. F. *J. Mol. Biol.* **1997**, *270*, 598−615.
(5) Shen, X.-C.; Liou, X.-Y.; Ye, L.-P.; Liang, H.; Wang, Z.-Y. *J. Colloid Interface Sci.* **2007**, *311*, 400−406.
(6) Lo, H. H.; Scaimmel, P. R. *J. Biol. Chem.* **1969**, *244*, 5084−5086.
(7) Li, R.; Nagai, Y.; Nagai, M. *J. Inorg. Biochem.* **2000**, *82*, 93−101.
(8) Kondo, A; Mihara, J. *J. Colloid Interface Sci.* **1996**, *177*, 214−221.
(9) Perutz, M. F.; Ladner, J. E.; Simon, S. R.; Ho, C. *Biochemistry* **1974**, *13*, 2163−2173.
(10) Ginger, R. G.; Zahn, D. P.; Brox, D. H.; Frund, H. E. *Eur. J. Biochem.* **1971**, *18*, 171−177.
(11) Zaroulis, C. G.; Kourides, I. A.; Valeri, C. R. *Blood* **1978**, *52*, 181−185.
(12) Bunn, H. F.; Briehl, R. W.; Larrabee, P.; Hobart, V. *J. Clin. Invest.* **1970**, *49*, 1088−1095.
(13) Ronda, L.; Bruno, S.; Viappiani, C.; Abbruzzetti, S.; Mozzarelli, A.; Lowe, K. C.; Bettati, S. *Protein Sci.* **2006**, *15*, 1961−1967.
(14) Sakurai, H.; Nagai, Y.; Nagai, M. *Biopolymers* **2004**, *74*, 60−63.
(15) DiIorio, E. E. *Methods Enzymol.* **1981**, *76*, 57−72.
(16) Winterbourn, C. C. *Methods Enzymol.* **1990**, *86*, 265−272.
(17) Lakowicz, J. R. *Principles of Fluorescence Spectroscopy*; Plenum Press: New York, 1983.
(18) Imoto, T.; Forster, L. S.; Rupley, J. A.; Tanaka, F. *Proc. Natl. Acad. Sci. U.S.A.* **1971**, *69*, 1151−1155.
(19) Mondal, M.; Chakrabarti, A. *FEBS Lett.* **2002**, *532*, 396−400.

(20) Chakraborty, D.; Bhattacharyya, M. *Mol. Cell. Biochem.* **2000**, *204*, 17−20.
(21) Chen, Y. H.; Yang, J. T.; Martinez, H. M. *Biochemistry* **1972**, *11*, 4120−4131.
(22) Lu, Z. X.; Cui, T.; Shi, Q. L. In *Molecular biology, applications of circular dichroism and optical rotatory dispersion*, 1st ed.; Science Press: Beijing, 1987.
(23) Park, S.-Y.; Yokoyama, T.; Shibayama, N.; Shiro, Y.; Tame, J. R. *J. Mol. Biol.* **2006**, *360*, 690−701.
(24) Morris, G. M.; Goodsell, D. S.; Halliday, R. S.; Huey, R.; Hart, W. E.; Belew, R. K.; Olson, A. J. *J. Comput. Chem.* **1998**, *19*, 1639−1662.
(25) Morris, G. M.; Goodsell, D. S.; Huey, R.; Olson, A. J. *J. Comput.-Aided Mol. Des.* **1996**, *10*, 293−304.
(26) Goodsell, D. S.; Olson, A. J. *Proteins: Struct., Funct., Genet.* **1990**, *8*, 195−202.
(27) DeLano, W. L. *The PyMOL*; Delano Scientific: San Carlos, CA, 2004; available at http://www.pymol.org.
(28) Trott, O.; Olson, J. O. *J. Comput. Chem.* **2009**, *31*, 455−461.
(29) Sheng, K.; Shariff, M.; Hebbel, R. P. *Blood* **1998**, *91*, 3467−3470.
(30) Burstein, E. A.; Vedenkina, N. S.; Ivkova, M. N. *Photochem. Photobiol.* **1973**, *18*, 263−279.
(31) Banerjee, M.; Maiti, S.; Kundu, I.; Chakrabarti, A.; Basu, S. *Photochem. Photobiol.* **2010**, *86*, 1237−1246.
(32) Banerjee, M.; Pal, U.; Subudhhi, A.; Chakrabarti, A.; Basu, S. *J. Photochem. Photobiol., B* **2012**, *108*, 23−33.
(33) Yang, X.; Chou, J.; Sun, G.; Yang, H.; Lu, T. *Microchem. J.* **1998**, *60*, 210−216.
(34) Venkateshrao, S.; Manoharan, P. T. *Spectrochim. Acta, Part A* **2004**, *60*, 2523−2526.
(35) Birner, G.; Albrecht, W.; Neumann, H.-G. *Arch. Toxicol.* **1990**, *64*, 97−102.
(36) Hsu, M - C.; Woody, R. W. *J. Am. Chem. Soc.* **1969**, *91*, 3679−3681.
(37) Brunori, M.; Antonini, E.; Wyman, J.; Anderson, S. R. *J. Mol. Biol.* **1968**, *34*, 357−359.